THE ASTROPHYSICAL JOURNAL, 283:33–49, 1984 August 1

SEVEN POOR CLUSTERS OF GALAXIES

TIMOTHY C. BEERS, MARGARET J. GELLER, JOHN P. HUCHRA, DAVID W. LATHAM, AND ROBERT J. DAVIS
Harvard-Smithsonian Center for Astrophysics[1]
Received 1983 September 15; accepted 1984 January 13

ABSTRACT

We have measured 83 new redshifts for galaxies in the region of seven of the poor clusters of galaxies identified by Morgan, Kayser, and White and Albert, White, and Morgan. For three systems (MKW 1s, AWM 1, and AWM 7) we have complete redshift samples for galaxies brighter than $m_{B(0)} = 15.7$ within 1° of the D or cD galaxy. We estimate masses for the clusters by applying both the virial theorem and the projected mass method. For each system, these two estimates, are consistent. Errors in these estimates, calculated with a statistical "jacknife" procedure, are in agreement with the analytic predictions of Bahcall and Tremaine.

For the two clusters (MKW 4 and AWM 7) with the highest X-ray luminosities, the line-of-sight velocity dispersions are ~ 700 km s^{-1}, and mass-to-light ratios $M/L_{B(0)} \gtrsim 400\ M_\odot/L_\odot$. For the five other clusters the velocity dispersions are $\lesssim 370$ km s^{-1}, and four of the five have mass-to-light ratios $\lesssim 250\ M_\odot/L_\odot$. The D or cD galaxy in each poor cluster is at the kinematic center of the system.

Medium resolution digital spectra of Ds and cDs in several X-ray clusters with radiative accretion flows all have Hα-[N II] emission systems. Similar spectra for the D galaxies in MKW 4 and AWM 7 show weak emission, consistent with the X-ray luminosities.

Subject headings: galaxies: clustering — galaxies: internal motions — galaxies: redshifts — X-rays: sources

I. INTRODUCTION

Morgan, Kayser, and White (1975, hereafter MKW) and Albert, White, and Morgan (1978, hereafter AWM) selected 23 poor clusters of galaxies on the basis of the D or cD-like appearance of the "first-ranked" galaxy. The poor clusters are physical systems (Stauffer and Spinrad 1978, 1980; Thomas and Batchelor 1978; Kriss *et al.* 1980; Schwartz *et al.* 1980; Kriss, Cioffi, and Canizares 1983, hereafter KCC) which contain 10–50 galaxies brighter than $m_3 + 2$ (m_3 is the magnitude of the third-ranked galaxy) within an Abell radius (Bahcall 1980).

There is considerable controversy about the photometric description (i.e., the existence or nonexistence of an extended halo above the extrapolated de Vaucouleurs $r^{-1/4}$ law) of the central galaxies in these clusters (Thuan and Romanishin 1981; Morbey and Morris 1983). Of the 11 poor clusters detected with the IPC on the *Einstein Observatory* (KCC), four (MKW 4, MKW 3s, AWM 4, and AWM 7) are sites of radiative accretion onto the D galaxy (KCC; Canizares, Stewart, and Fabian 1983).

We analyze complete redshift samples for three poor clusters MKW 1s, AWM 1, and AWM 7. The samples include redshift measurements for all galaxies in the Zwicky catalog ($m_{B(0)} \leq 15.7$; Zwicky *et al.* 1961–1968) within 1° of the D galaxy in each system. We supplement our velocity data by searching a master redshift catalog (Huchra 1984) over a 5° region surrounding each of the clusters; with these data we derive dynamical parameters for four more poor clusters—MKW 1, MKW 4, MKW 12, and AWM 3. The more extended velocity sample is particularly useful for detecting interlopers (galaxies accidentally superposed on the cluster region). Kriss (1983) is also accumulating velocity data for some of these systems.

[1] Research reported here based in part on observations at the Multiple Mirror Telescope Observatory, a joint facility of the Smithsonian Institution and the University of Arizona.

In § II we list 83 new redshifts for galaxies in the seven MKW-AWM poor clusters, and we summarize the available data within the 5° regions. We derive dynamical parameters for the clusters in § III and demonstrate a new method for estimating errors in the mass-to-light ratios. Four clusters have mass-to-light ratios less than $M/L_{B(0)} \approx 250\ M_\odot/L_\odot$ ($H_0 = 100$ km s^{-1} Mpc^{-1}). The two clusters with the highest X-ray luminosities have $M/L_{B(0)} \gtrsim 400\ M_\odot/L_\odot$.

We demonstrate that the D galaxy always lies at the kinematic center of the cluster. This analysis supports the conclusions drawn from observations of cooling flows in the X-ray. In § IV we show medium resolution (6–7 Å) digital spectra for several cDs with cooling flows and associated emission systems detected by Cowie *et al.* (1983) and Heckman (1981). Equivalent widths of the Hα-[N II] emission lines in these spectra confirm the previous detections. The spectra of the Ds in two poor clusters with cooling flows have Hα-[N II] equivalent widths which are consistent with those expected for their X-ray luminosities.

II. OBSERVATIONS

Optical redshifts of 80 galaxies were measured with the photon-counting Reticon detector system ("*Z*-machine"; Latham 1982) on the 1.5 m telescope at the Whipple Observatory. Fifty of the new redshifts are for galaxies in three poor clusters (MKW 1s, AWM 1, and AWM 7) for which we have complete redshift surveys within a 1° radius and to a limiting magnitude $m_{B(0)} = 15.7$. Velocities were obtained as in the CfA redshift survey (Huchra *et al.* 1983) and have a mean external error of ~ 30 km s^{-1}. Redshifts for three galaxies were measured with the MMT spectrograph at somewhat lower resolution (9 Å) with a mean external error of ~ 100 km s^{-1} (Beers 1983). Because we expect the velocity dispersions of the poor clusters to be $\lesssim 500$ km s^{-1}, and because the number of galaxies in each system is small, the $\lesssim 50$ km s^{-1} errors in typical *Z*-machine velocities are important for the estimation of dynamical parameters.

TABLE 1

Coordinates, Magnitudes, and Velocities for Galaxies in Poor Clusters

Name (1)	5° Identification (2)	R.A. (1950) (3)	Decl. (1950) (4)	$m_{B(0)}$ (5)	cz_h (6)	Error (7)	Reference (8)
		MKW 1 (40 galaxies)					
NGC 2974	1	9 40.0	−3 28	12.3	1998	26	0
0940−0201	2B	9 40.5	−2 1	14.7	4500	220	5
0940−0504	3	9 40.9	−5 4	...	1951	52	0
0941−0025	4	9 41.5	−0 25	15.5	1402	20	37
0941−0026	5	9 41.6	−0 26	15.4	1495	60	37
0944+0044	6	9 44.3	0 44	15.3	1787	20	2
0945−0148	7	9 45.0	−1 48	15.5	1425	25	2
NGC 3015	8 B	9 46.8	1 22	14.2	7500	22	1
NGC 3018	9	9 47.1	0 51	14.2	1874	14	37
NGC 3023	10	9 47.3	0 51	13.5	1848	20	6
0949+0141	11	9 49.2	1 41	...	1853	10	2
0949−0145	12 B	9 49.6	−1 45	...	5747	36	T
0949−0122	13 B	9 49.7	−1 22	...	6108	41	T
NGC 3044	14	9 51.1	1 48	12.5	1335	24	0
0954−0210	15	9 54.8	−2 10	15.7	14330	38	T
0957−0155	16	9 57.2	−1 55	15.5	11307	39	T
NGC 3083	17 A	9 57.3	−2 38	14.2	6318	48	T
NGC 3086	18 A	9 57.6	−2 44	14.5	6703	35	T
NGC 3090 ⟨——⟩ .	19 A	9 58.0	−2 43	14.1	6057	39	27
0958−0155	20 A	9 58.0	−1 55	14.3	6117	30	T
0958−0242	21 A	9 58.2	−2 42	15.5	6024	28	T
NGC 3092	22 A	9 58.3	−2 46	14.5	5893	42	T
NGC 3093	23 A	9 58.4	−2 43	15.1	6139	29	T
0958+0009	24	9 58.6	0 9	...	13790	20	37
0958+0006	25	9 58.6	0 6	...	26800	20	37
1000−0546	26	10 0.2	−5 46	...	666	15	2
1001−0210	27 A	10 1.9	−2 10	14.6	5953	34	T
NGC 3115	28	10 2.7	−7 28	10.4	698	6	0
IGC 590A	29 B	10 3.3	0 53	15.0	6246	33	T
IGC 590B	30 B	10 3.3	0 53	15.0	6365	30	T
IGC 592	31 B	10 5.4	−2 15	14.0	6016	33	T
IGC 593	32 B	10 5.8	−2 17	14.2	6010	35	T
IG 594	33 B	10 6.0	0 25	14.7	6449	33	T
1008−0428	34	10 8.6	−4 28	12.3	324	10	1
1008+0012	35	10 8.6	0 12	15.5	10087	35	T
1008+0013	36	10 8.8	0 13	15.4	10163	38	T
1008+0019	37	10 8.7	0 19	15.6	9916	33	T
1008+0041	38	10 8.8	0 41	14.0	3636	10	9
1011−0041	39	10 11.1	−0 41	14.4	13293	29	27
IGC 600.............	40	10 14.7	−3 15	13.3	1314	15	2
		MKW 4 (53 galaxies)					
1145+0446	1 B	11 45.4	4 46	14.4	5981	31	27
NGC 3907B	2 B	11 46.8	−0 48	14.8	6560	64	37
NGC 3907A	3 B	11 46.9	−0 48	14.4	6206	59	37
1147−0019	4	11 47.8	−0 19	...	41670	200	37
1147−0018A	5	11 47.8	−0 18	...	51440	200	37
1147−0018B	6	11 47.8	−0 18	...	41490	200	37
1150+0201	7 B	11 50.2	2 1	14.4	6118	35	27
IGC 745	8	11 51.7	0 25	13.7	1050	150	5
1152+0627	9 B	11 52.6	6 27	14.5	6973	25	0
1153+0132	10	11 53.1	1 32	14.1	1894	15	2
1156−0110A	11	11 56.2	−1 10	14.6	1481	11	37
1156−0110B	12 B	11 56.2	−1 10	...	6348	25	37
NGC 4030	13	11 57.8	−0 49	11.6	1463	15	2
1158+0015	14	11 58.2	0 15	17.0	1937	10	0
1158−0100	15	11 58.6	−1 0	14.4	1519	45	T
1159+0606	16	11 59.2	6 6	14.9	1320	300	37
NGC 4043	17 B	11 59.8	4 37	14.1	6462	25	27
NGC 4045	18	12 0.2	2 16	13.1	1942	20	27
NGC 4045A	19 A	12 0.2	2 14	15.2	4892	75	21
1200+0214	20 A	12 0.7	2 14	14.7	5976	75	21
1200+0219	21 A	12 0.9	2 19	...	5612	75	21
1201+0220	22 A	12 1.1	2 20	14.8	6007	75	21
1201+0207	23 A	12 1.2	2 7	...	4991	75	21
NGC 4058	24 B	12 1.2	3 50	14.0	5800	22	27
1201+0211	25 A	12 1.4	2 11	15.4	5382	75	21

TABLE 1—*Continued*

Name (1)	5° Identification (2)	R.A. (1950) (3)	Decl. (1950) (4)	$m_{B(0)}$ (5)	cz_h (6)	Error (7)	Reference (8)
NGC 4063	26 A	12 1.5	2 8	15.0	5876	75	21
1201+0207	27 A	12 1.6	2 7	15.5	6642	75	21
1201−0115	28	12 1.8	−1 15	...	1463	15	2
1201+0208	29 A	12 1.8	2 8	15.3	6662	75	21
NGC 4073 ⟨——⟩ .	30 A	12 1.9	2 11	12.7	5966	20	27
IGC 2989	31 A	12 2.0	2 5	14.8	5588	24	T
NGC 4077	32 A	12 2.1	2 4	14.5	7030	20	27
NGC 4075	33 A	12 2.1	2 21	14.7	6560	25	T
NGC 4079	34 B	12 2.3	−2 5	14.0	6067	29	T
NGC 4116	35	12 5.1	2 58	12.7	1323	10	0
1205−0049	36	12 5.1	−0 49	...	91800	300	37
NGC 4123	37	12 5.6	3 10	12.0	1328	10	6
1208+0217	38	12 8.5	2 17	...	1339	10	2
1208+0312	39	12 8.9	3 12	15.5	1297	10	0
NGC 4179	40	12 10.3	1 35	12.2	1239	34	27
NGC 4197	41	12 12.0	6 5	13.8	2082	38	27
1212+0602	42	12 12.8	6 2	15.4	2043	31	T
1214+0424	43	12 14.2	4 24	...	22920	200	10
NGC 4234	44	12 14.6	3 58	13.6	2075	66	0
1214+0353	45	12 16.9	3 53	...	23220	200	37
1215+0356	46	12 15.1	3 56	...	22770	200	37
1215+0043	47	12 15.4	0 43	15.4	941	15	2
1215+0119	48	12 15.9	1 19	...	35000	300	37
NGC 4255	49	12 16.4	5 4	13.5	1696	50	13
1216+0408	50	12 16.6	4 8	14.5	1582	39	0
NGC 4292	51	12 18.7	4 52	14.1	2258	25	27
1220+0257	52 B	12 20.7	2 57	...	7013	100	3
1220+0154	53	12 20.9	1 54	...	8230	100	10
		MKW 12 (75 galaxies)					
1344+1153A	1	13 44.4	11 53	15.1	10656	15	37
1344+1153B	2	13 44.5	11 53	...	10670	10	37
1345+1232	3	13 45.1	12 32	...	36520	300	37
1345+0738A	4 B	13 45.6	7 38	14.7	6956	30	37
1345+0738B	5 B	13 45.7	7 38	14.9	7072	15	37
NGC 5338	6	13 50.9	5 27	14.3	777	29	27
NGC 5348	7	13 51.7	5 29	14.5	1457	15	2
NGC 5356	8	13 52.4	5 35	14.1	1397	35	27
NGC 5360	9	13 53.1	5 14	14.9	1177	31	0
IGC 959	10 B	13 53.6	13 45	14.4	6872	27	27
NGC 5363	11	13 53.6	5 30	11.5	1138	41	1
NGC 5364	12	13 53.7	5 16	11.3	1256	20	1
1354+1215	13 B	13 54.7	12 15	14.9	6160	24	T
IGC 962	14 B	13 54.7	12 16	14.0	6192	20	27
NGC 5374	15 B	13 55.0	6 21	13.7	4295	31	27
1355+1007	16 A	13 55.4	10 7	14.5	6833	10	16
NGC 5384	17 B	13 55.7	6 46	14.0	5103	22	27
NGC 5382	18 B	13 55.7	6 30	14.0	4312	23	27
NGC 5386	19 B	13 55.8	6 35	13.7	4296	27	3
1356+1424	20	13 56.2	14 24	...	24520	300	37
1356+0858	21	13 56.5	8 58	...	12140	300	37
1357+0912	22 A	13 57.8	9 12	14.8	4106	10	16
1357+1312	23	13 57.9	13 12	15.5	480	114	33
1358+0853	24 A	13 58.0	8 53	15.6	4609	15	32
NGC 5405	25 B	13 58.7	7 57	14.5	6922	39	27
1358+1022	26 A	13 58.8	10 22	15.3	6844	6	32
1358+1043	27	13 58.9	10 43	15.2	10241	52	T
NGC 5409	28 A	13 59.3	9 43	14.4	6259	5	32
1359+0901	29 A	13 59.4	9 1	14.7	6066	6	32
NGC 5411	30 A	13 59.5	9 11	14.6	5850	100	15
NGC 5414	31 A	13 59.6	10 10	13.8	4279	20	16
NGC 5416	32 A	13 59.7	9 40	13.6	6230	6	32
NGC 5417	33 A	13 59.7	8 17	13.8	4817	21	27
NGC 5418	34 B	13 59.8	7 56	14.4	4544	36	27
1400+0919	35 A	14 0.1	9 19	15.0	5992	11	32
1400+0924	36 A	14 0.2	9 24	15.7	5854	22	32
NGC 5423	37 A	14 0.3	9 35	13.9	5750	28	27
1400+0901	38 A	14 0.4	9 1	15.6	5858	23	32
NGC 5424 ⟨——⟩ .	39 A	14 0.5	9 40	14.2	6026	25	27
NGC 5431	40 A	14 0.6	9 37	14.8	5745	100	15

TABLE 1—*Continued*

Name (1)	5° Identification (2)	R.A. (1950) (3)	Decl. (1950) (4)	$m_{B(0)}$ (5)	cz_h (6)	Error (7)	Reference (8)
NGC 5434A	41 A	14 0.9	9 41	14.3	4634	10	32
NGC 5434B	42 A	14 1.0	9 43	14.7	5632	5	32
NGC 5436	43 A	14 1.2	9 49	14.9	6614	200	15
NGC 5438	44 A	14 1.3	9 51	14.7	7066	100	15
1401+0458	45	14 1.9	4 58	...	8780	300	37
NGC 5454	46	14 2.3	14 37	14.4	7681	23	27
1402+0903	47	14 2.4	9 3	14.9	1233	15	2
1402+1258	48 B	14 2.4	12 58	15.3	4200	150	5
NGC 5456	49 B	14 2.5	12 7	14.2	7147	34	27
NGC 5459	50 B	14 2.5	13 22	14.5	5261	27	27
1402+0934	51 A	14 2.6	9 34	15.6	4600	10	16
1403+0909	52 A	14 3.1	9 9	15.3	7044	10	16
1403+0915	53 A	14 3.5	9 15	15.2	7001	10	16
NGC 5463	54 A	14 3.7	9 36	14.1	7235	25	27
NGC 5470	55	14 4.0	6 16	14.5	1023	33	27
1404+0933	56 A	14 4.4	9 33	15.4	7208	10	16
1404+0828	57	14 4.4	8 28	...	13790	300	37
1404+0626	58 B	14 4.5	6 28	...	7410	300	37
1405+1004	59	14 5.5	10 4	...	26080	300	37
1406+0718	60 B	14 6.0	7 18	14.5	5929	38	27
NGC 5482	61 A	14 6.0	9 10	14.2	7100	22	27
NGC 5491	62	14 8.5	6 36	13.9	727	100	9
NGC 5505	63 B	14 10.1	13 32	14.1	4272	29	27
NGC 5514	64 B	14 11.2	7 54	14.5	7343	30	27
1411+1244	65 B	14 11.2	12 44	14.4	5909	31	27
NGC 5531	66 B	14 14.3	11 7	14.7	7825	40	T
1414+0954	67	14 14.4	9 54	...	25180	300	37
NGC 5532	68 B	14 14.4	11 2	13.3	7367	24	27
1415+0825	69	14 15.1	8 25	...	17421	28	T
NGC 5542	70 B	14 15.4	7 47	15.0	7765	22	T
NGC 5546	71 B	14 15.7	7 48	14.1	7324	29	27
IGC 993	72	14 15.8	11 27	15.4	18600	200	5
NGC 5549	73 B	14 16.1	7 36	14.2	7731	29	27
1417+0936	74	14 17.3	9 36	14.7	1281	10	2
NGC 5562	75	14 17.7	10 29	14.5	9139	28	27
		MKW 1s (19 galaxies)					
0900+0334	1	9 0.8	3 34	15.2	7935	60	37
0901+0334	2 B	9 1.0	3 34	15.1	3694	60	37
NGC 2765	3 B	9 5.0	3 35	13.3	3827	30	37
0914+0047	4	9 14.3	0 47	15.5	8543	100	T
0915+0115	5	9 15.2	1 15	15.7	8317	71	T
0917+0109	6 A	9 17.3	1 9	15.4	5325	35	T
0917+0108	7 A	9 17.4	1 8	15.5	5255	49	T
0917+0116 ⟨——⟩.	8 A	9 17.5	1 16	13.8	5151	26	27
0920+0138	9 A	9 20.4	1 38	15.4	5232	35	T
0920+0147	10	9 20.8	1 47	15.6	7782	53	T
NGC 2861	11 B	9 21.0	2 20	14.0	5134	15	9
0921+0133	12	9 21.1	1 33	14.8	7685	100	T
NGC 2877	13 B	9 23.2	2 36	14.7	6900	200	5
NGC 2900	14 B	9 27.7	4 22	14.6	5343	8	6
0931+0029	15 B	9 31.6	0 29	13.9	4813	20	37
0931+0030	16 B	9 31.6	0 30	...	4715	28	37
0934+0120	17	9 34.5	1 20	15.4	14939	100	5
NGC 2936	18 B	9 35.1	2 58	14.4	6981	37	0
NGC 2937	19 B	9 35.1	2 58	15.0	6990	34	0
		AWM 1 (56 galaxies)					
0900+1827	1	9 0.4	18 27	...	3269	200	37
0900+2052	2 B	9 0.6	20 52	...	9457	200	37
NGC 2738	3	9 1.1	22 10	13.8	3102	15	6
NGC 2744	4	9 1.8	18 40	14.2	3431	10	6
NGC 2749	5	9 2.5	18 31	13.7	4180	21	27
NGC 2752	6	9 2.9	18 32	14.8	4022	71	33
0904+1651	7	9 4.6	16 51	...	22660	200	37
0904+1650	8	9 4.7	16 50	...	23680	200	37
NGC 2764	9	9 5.4	21 39	13.9	2707	14	1
IGC 528A	10	9 6.6	15 59	14.6	3808	29	T
IGC 528B	11	9 6.6	15 59	...	6333	41	T

TABLE 1—*Continued*

Name (1)	5° Identification (2)	R.A. (1950) (3)	Decl. (1950) (4)	$m_{B(0)}$ (5)	cz_h (6)	Error (7)	Reference (8)
IGC 528C	12 B	9 6.6	15 59	...	8635	45	T
IGC 2441	13	9 7.1	23 3	15.3	12134	32	T
0910+2035	...	9 10.2	20 35	15.3	...		
0910+1751	14 B	9 10.5	17 51	15.1	7710	92	0
0910+2046	15 A	9 10.9	20 46	15.4	8450	33	T
0911+1657	16 B	9 11.4	16 57	14.7	8362	15	0
0912+2020	17 A	9 12.0	20 20	15.7	9628	56	T
NGC 2790	18 A	9 12.2	19 55	14.7	7874	33	T
IGC 2453	19 A	9 13.0	21 9	15.5	9025	34	T
NGC 2802	20 B	9 13.9	19 10	15.0	8783	27	T
NGC 2803	21 B	9 13.9	19 10	15.0	8896	37	T
0913+2003	22 A	9 13.9	20 3	15.6	8662	34	T
NGC 2801	23 A	9 13.9	20 8	15.4	7767	41	T
NGC 2804 ⟨——⟩ .	24 A	9 14.0	20 24	14.2	8424	23	27
NGC 2806	25 B	9 14.1	20 15	...	8170	100	21
NGC 2807A	26 A	9 14.2	20 14	15.1	8312	35	T
NGC 2807B	27 A	9 14.2	20 14	15.1	8059	33	T
0914+2005	28 A	9 14.3	20 5	15.6	8690	35	T
NGC 2809	29 A	9 14.3	20 16	13.9	8299	31	T
0914+2021	30 A	9 14.4	20 21	15.0	9135	37	T
0914+2004	31 A	9 14.7	20 4	15.7	9340	34	T
NGC 2812	32 A	9 14.8	20 7	15.7	9048	32	T
NGC 2813	33 A	9 14.9	20 6	15.4	8678	40	T
0915+2041	34 A	9 15.1	20 41	15.6	9086	32	T
0915+2035	35 A	9 15.4	20 35	15.7	9548	28	T
0915+2028	36 A	9 15.5	20 28	15.5	8357	34	T
0915+1631	37 B	9 15.6	16 31	15.2	8691	100	3
0915+2037	38 A	9 15.6	20 37	15.7	9572	35	T
0915+2057	39 A	9 15.9	20 57	15.6	9106	39	T
0916+2022	40 A	9 16.0	20 22	15.7	8782	33	T
0916+2056	41 A	9 16.0	20 56	15.6	9191	34	T
0916+2027	42 A	9 16.4	20 27	15.4	9040	35	T
0916+1950	43 A	9 16.7	19 50	15.5	10431	42	T
0921+1722	44	9 21.0	17 22	15.2	12930	100	37
0921+1802	45	9 21.4	18 2	16.5	23076	200	5
0921+1753	46	9 21.9	17 53	14.9	4195	200	5
0923+1936	47	9 23.2	19 36	14.4	2534	35	T
0925+1725	48	9 25.3	17 25	14.5	4215	30	27
0925+2045	49	9 25.7	20 45	...	57612	100	37
IGC 2489	50	9 27.3	20 17	14.2	4294	39	27
0927+1635	51 B	9 27.6	16 35	15.5	8613	20	37
NGC 2903	52	9 29.3	21 43	9.7	539	26	27
0930+2145	53	9 30.0	21 45	...	448	10	30
0930+2321	54 B	9 30.4	23 21	15.3	7800	200	5
NGC 2916	55	9 32.1	21 56	12.3	3695	20	6
0934+2003	56 B	9 34.4	20 3	14.3	8461	30	27
		AWM 3 (44 galaxies)					
1410+2928A	1	14 10.7	29 28	...	76100	300	37
1410+2928B	2	14 10.7	29 28	...	66500	300	37
NGC 5523	3	14 12.6	25 33	12.6	1048	10	2
1413+2317	4	14 13.6	23 17	15.3	153	5	2
1415+2705A	5	14 15.1	27 5	...	10767	32	5
1415+2705B	6	14 15.1	27 5	...	10933	54	5
IGC 4397	7 B	14 15.7	26 39	14.2	4410	31	27
NGC 5548	8 B	14 15.7	25 22	13.5	4980	8	0
NGC 5553	9 B	14 16.2	26 31	14.8	4539	27	T
1416+2203	10 B	14 16.4	22 3	15.4	2550	200	5
IGC 4405	11	14 16.9	26 32	14.9	11025	14	37
1417+2632	12	14 17.0	26 32	15.7	11093	14	37
1418+2210	13 B	14 18.4	22 10	14.7	4649	20	6
1422+2755	14	14 22.0	27 55	...	10109	50	37
NGC 5610	15 A	14 22.1	24 50	14.5	5087	26	27
1422+2651	16	14 22.4	26 51	15.6	10171	70	0
1422+2622	17	14 22.6	26 22	15.7	10200	21	19
1425+2132	18	14 25.6	21 32	...	1043	50	37
1425+2604	19 A	14 25.6	26 4	15.4	4219	48	T
IGC 1017	20 A	14 25.9	26 5	14.9	4392	21	T
NGC 5629 ⟨——⟩ .	21 A	14 26.1	26 4	14.1	4495	30	27
1426+2729	22 A	14 26.3	27 29	15.3	3819	174	0

TABLE 1—*Continued*

Name (1)	5° Identification (2)	R.A. (1950) (3)	Decl. (1950) (4)	$m_{B(0)}$ (5)	cz_h (6)	Error (7)	Reference (8)
NGC 5635	23 A	14 26.3	27 38	13.9	4352	27	27
1426+2728	24 A	14 26.6	27 28	...	4440	200	5
NGC 5642	25 B	14 27.0	30 15	14.3	4355	26	27
NGC 5641	26 B	14 27.1	29 3	13.0	4346	23	27
NGC 5657	27 B	14 28.5	29 24	14.4	3911	30	27
1428+2551	28	14 28.8	25 51	...	27228	37	27
1428+2830	29	14 28.8	28 30	15.1	13590	200	5
1428+2727	30 A	14 28.9	27 27	15.2	4512	200	3
1430+2508	31	14 30.5	25 8	...	24300	250	37
1434+2501	32	14 34.9	25 1	...	25840	200	37
1435+2458	33	14 35.0	24 58	...	26140	200	37
1435+2503	34	14 35.3	25 3	...	27160	200	37
1435+2500	35	14 35.4	25 0	...	26920	200	37
1435+2504	36	14 35.6	25 4	...	25960	200	37
NGC 4479	37	14 36.5	28 43	14.8	13641	36	T
1438+2850A	38	14 38.9	28 50	...	74300	300	37
1438+2850B	39	14 38.9	28 50	...	74000	300	37
1438+2850C	40	14 38.9	28 50	...	42200	300	37
NGC 5735	41 B	14 40.2	28 56	13.8	3744	15	9
1441+2613	42	14 41.9	26 13	...	18540	250	37
1448+2623A	43	14 48.0	26 23	...	35084	60	37
1448+2623B	44	14 48.0	26 23	...	35506	60	37
			AWM 7 (33 galaxies)				
0246+4116	15 A	2 46.6	41 16	14.7	5285	53	T
0246+4111	16 A	2 46.9	41 11	15.7	5769	36	T
NGC 1106	17 A	2 47.4	41 29	13.7	4230	38	T
0249+4112	19 A	2 49.4	41 12	14.9	4305	65	37
0249+4122	20 B	2 49.4	41 22	...	4524	65	37
0249+4111	21 B	2 49.5	41 11	...	3924	65	37
NGC 1122	22 A	2 49.6	42 0	13.0	3704	27	T
0249+4120	23 A	2 49.8	41 20	15.6	6782	40	T
0250+4142	24 A	2 50.3	41 42	14.4	7156	65	37
0250+4132	25 A	2 50.4	41 32	15.7	6149	65	37
0250+4116	26 B	2 50.6	41 16	...	4581	65	37
0250+4133	27 B	2 50.7	41 33	...	4510	150	21
0251+4111	28 B	2 51.1	41 11	...	6030	200	21
NGC 1129A	29 B	2 51.2	41 22	...	5055	24	T
NGC 1130	30 A	2 51.2	41 25	15.6	6163	22	T
NGC 1129 ⟨——⟩ .	32 A	2 51.3	41 23	12.4	5268	20	27
0251+4128	33 B	2 51.3	41 28	...	5650	100	21
NGC 1131	34 A	2 51.4	41 22	15.6	5348	23	T
0251+4120	35 A	2 51.5	41 20	14.8	4455	26	27
IGC 265	36 A	2 51.5	41 28	15.7	5296	28	T
0251+4140	37 A	2 51.5	41 40	15.7	5804	65	37
0251+4112	38 B	2 51.5	41 12	...	5460	200	21
0251+4107	39 A	2 51.6	41 7	15.1	5825	65	37
0251+4125	40 B	2 51.7	41 25	...	4195	29	T
0251+4124	41 B	2 51.8	41 24	...	4026	65	37
IGC 266	...	2 51.8	42 05	15.7	...		
0252+4132	42 B	2 52.7	41 32	...	6607	65	37
0252+4122	43 A	2 52.7	41 22	15.2	4710	65	37
0252+4126	44 A	2 52.9	41 26	15.6	5996	65	37
0253+4108	45 B	2 53.4	41 8	...	4605	65	37
0254+4120	46 A	2 54.3	41 20	15.3	4893	27	T
0255+4106	47 B	2 55.7	41 6	...	4920	60	37
0255+4105	48 A	2 55.8	41 5	15.5	5075	28	T
0256+4111	50 A	2 56.3	41 11	15.4	5675	41	T

NOTES.—Numbered references are as in Huchra *et al.* 1983, (10) Bohuski, Fairall, and Weedman 1978; (19) Colla *et al.* 1975; (30) Thuan and Seitzer 1979; (37) Palumbo, Tanzella-Nitti, and Vettolani 1982.

To extend the data set, we use a redshift catalog (Huchra 1984) which lists the best available redshifts for over 13,000 galaxies. We have assembled enough redshifts for dynamical studies of seven poor clusters: the samples for four of the systems are incomplete. The data are in Table 1. Column (1) is the galaxy name, column (2) the reference number in the 5° sample, columns (3) and (4) the 1950 equatorial coordinates, taken in most cases from the Zwicky catalog, and column (5) the $B(0)$ magnitude from either the *Reference Catalogue of Bright Galaxies* (de Vaucouleurs and de Vaucouleurs 1964) or from the Zwicky catalog. The magnitudes of the D galaxies (denoted in the table by "$\langle$——$\rangle$") are from Thuan and Romanishin (1981), corrected to $B(0)$ using $B(0) = B_T + 0.4$ (Huchra 1976). Column (6) is the heliocentric velocity (cz_h) in kilometers per second, and column (7) is the estimated *external* error in kilometers per second. Column (8) is the velocity reference, with source codes as in Huchra *et al.* (1983): "T" indicates a new redshift. For AWM 7, many velocities for galaxies within 5° of NGC 1129 are in the literature (Kent and Sargent 1983). Only the galaxies within 1° of NGC 1129 are listed in Table 1.

III. DYNAMICS

Our goal is to obtain velocity dispersions and mass-to-light ratios for the seven systems. We also use the velocity data for an independent confirmation of the X-ray evidence (Canizares, Stewart, and Fabian 1983) that the D galaxies are nearly stationary in the bottom of the cluster potential well. The systems fall into two groups: (1) those for which we have complete velocity samples, and (2) those for which we have culled incomplete velocity data from the literature.

a) Analysis of Complete Samples

Figure 1 is a set of cone diagrams in right ascension and heliocentric velocity (cz_h) for the three systems (MKW 1s, AWM 1, and AWM 7) with complete redshift data. The dotted lines mark the 1° field; the open circles denote galaxies in the magnitude-limited sample. The dashed lines mark the range of velocities within ± 2000 km s^{-1} of the D galaxy. Galaxies with extreme velocities have been removed. The pronounced finger to the left in the cone diagram for AWM 7 is the core of the Perseus cluster.

On the basis of the spatial and velocity information we select two mutually exclusive subsamples for further analysis. Both subsamples of galaxies lie within the velocity limits shown by the dashed lines on the cone diagrams. The subsamples A and B are as follows:

A: Galaxies *within* a 1° radius of the D galaxy and brighter than $m_{B(0)} = 15.7$ ("complete sample"; open circles in Fig. 1).

B: Galaxies *outside* the 1° region but *within* a region of 5° radius, *and* galaxies fainter than $m_{B(0)} = 15.7$ over the entire 5° region (closed circles).

Sample B gives us added confidence in the rejection of interlopers and in the determination of the velocity dispersion.

For each poor cluster we estimate the mean velocity, the line-of-sight velocity dispersion, and the mass-to-light ratio. (The procedure for estimating the velocity dispersion and its error is described fully in Danese, De Zotti, and di Tullio 1980). Table 2 contains the $B(0)$ and X-ray luminosities for each cluster. Column (1) is the cluster name, column (2) the number of galaxies in sample A, and column (4) is the summed $B(0)$ luminosity for the cluster members in sample A corrected for galactic absorption and K-dimming (col. [3]: Sandage 1973; Coleman, Wu, and Weedman 1980). Column (8) gives the luminosity correction for the contribution from galaxies fainter than the survey limit (using the luminosity function from the CfA redshift survey; Davis and Huchra 1982). Columns (5), (6), and (7) are completeness correction factors for the incompletely sampled clusters discussed in § III*b*. The total $B(0)$ luminosity corrected for incomplete sampling is in column (9), and the X-ray luminosity is in column (10).

There are two estimates of the mass within the 1° region. The virial mass is

$$M_{\rm vt} = \frac{3\pi}{G}\,\sigma_r{}^2 \left\langle \frac{1}{r} \right\rangle^{-1}, \tag{1}$$

where

$$\left\langle \frac{1}{r} \right\rangle^{-1} = \frac{D}{2}\,N(N-1)\left(\sum_i \sum_{j<i} \frac{1}{\theta_{ij}}\right)^{-1},$$

θ_{ij} is the angular separation of galaxies i and j, D the radial distance, and N is total number of galaxies. Note that the mean harmonic radius $\langle 1/r \rangle^{-1}$ is limited by the resolution of the Zwicky catalog ($\sim\frac{1}{2}$ the nominal position error of 1′). In only one case (AWM 1) do we include a pair of galaxies with pro-

TABLE 2

$B(0)$ AND X-RAY LUMINOSITIES

Cluster (1)	$N_{\rm A}$ (2)	$A_{\rm B} + K_{\rm B}$ (3)	L_m[a] (4)	L_i[a] (5)	L_u[a] (6)	f_1 (7)	f_2 (8)	$L_{B(0)}$[a] (9)	L_x (10^{42} ergs s^{-1}) (10)
				Complete					
MKW 1s	4	0.19	0.24	0.14	...	...	1.6	0.37	0.15
AWM 1	12	0.20	1.6	0.93	0.10	...	2.9	4.5	...
AWM 7	20	0.49	2.4	...	0.04	...	1.9	4.7	40.0
				Incomplete					
MKW 1[b]	8	0.18	0.81	0.08	0.35	0.91	1.8	2.1	<0.21
MKW 4	13	0.10	1.2	0.62	1.3	0.66	1.8	3.7	5.8
MKW 12 ...	11	0.10	1.2	1.3	1.4	0.48	1.8	3.3	0.12
AWM 3	8	0.07	0.35	0.04	0.90	0.90	1.4	1.7	<0.17

[a] Times 10^{11} $L_\odot$.

[b] Missing roughly one-third of sample region due to declination cutoff of Zwicky catalog.

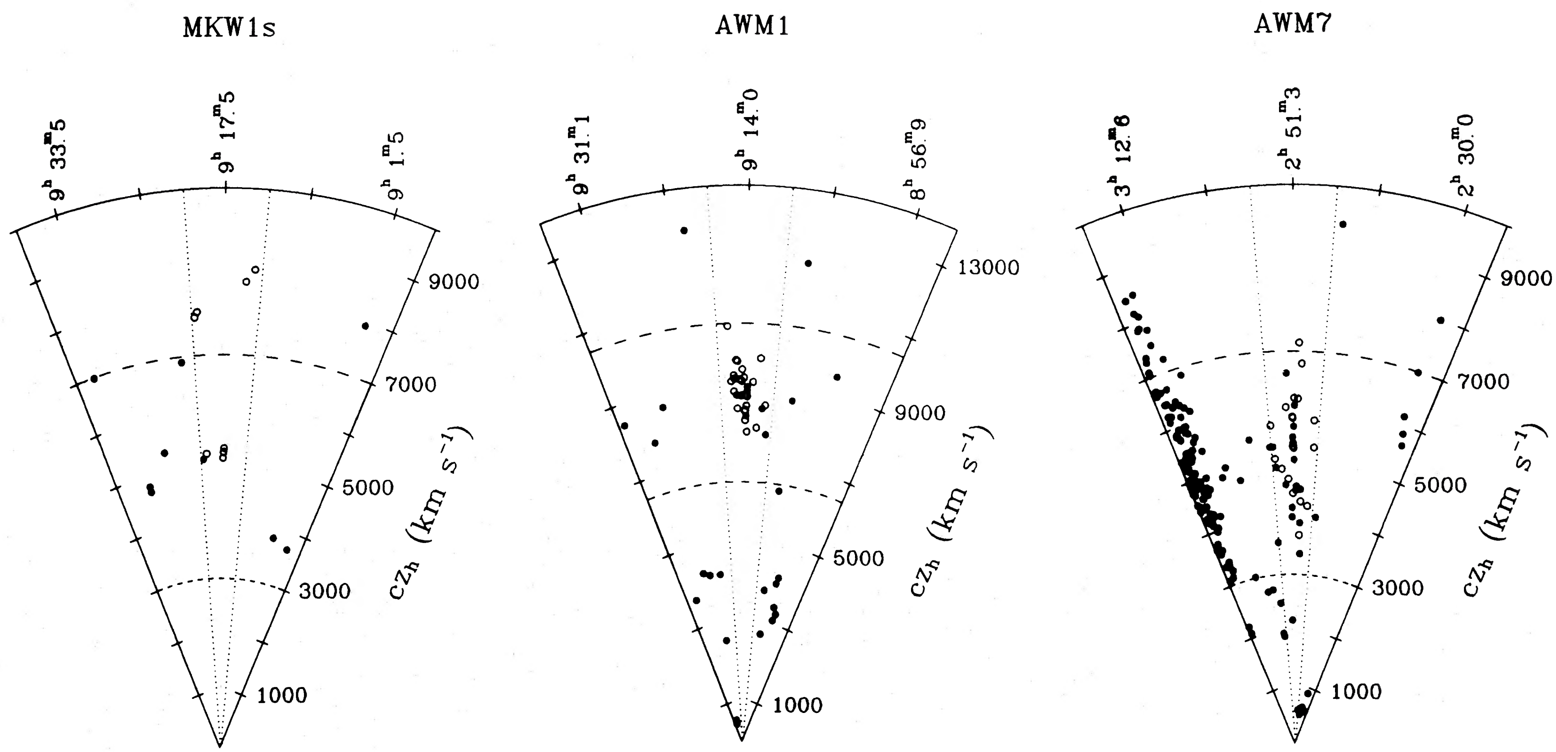

FIG. 1.—Heliocentric velocity (cz_h); right ascension cone diagrams for completely surveyed systems. Dotted lines mark the 1° regions of the complete survey; open circles are the galaxies brighter than $m_{B(0)} = 15.7$. Dashed lines are the velocity limits for the dynamical analysis.

jected separation less than the resolution of the Zwicky catalog. The projected mass (Bahcall and Tremaine 1981) is

$$M_{\mathrm{pm}} = \frac{24}{\pi G N} \sum_i v_i^2 R_i \,, \tag{2}$$

where R_i is the projected distance of galaxy i from the D galaxy, v_i is the velocity of galaxy i with respect to the velocity of the D, and $N + 1$ is the total number of galaxies in the cluster (including the D). The projected mass estimate in equation (2) applies to N test particles moving about a central mass concentration. This estimate may be well suited to these poor clusters because both X-ray and optical evidence (§ IV) show that the D galaxy defines the center of mass of the system. The projected mass estimate can be biased upward by velocity interlopers, particularly those at large distances from the assumed center. Because of its sensitivity to the relative positions of galaxies in the system, the virial theorem estimate can be severely biased downward by an interloper which lies near a group member.

We estimate the errors in the dynamical quantities with the statistical "jacknife" (Diaconis and Efron 1983). We calculate dynamical parameters for all subsets of $N - 1$ galaxies (where, for the virial theorem, N is the total number of galaxies in the system, and, for the projected mass estimate, N is the number of members excluding the D). For any parameter, the error is the standard deviation about the mean value for the N subsets. Bahcall and Tremaine (1981) show that the fractional standard deviation in the virial estimator is always *at least* as large as $\pi^{-1}(2 \ln N)^{1/2} N^{-1/2}$ as $N \to \infty$; the fractional standard deviation in the projected mass estimator is $\sim 1.4 N^{-1/2}$. The jacknife error estimates agree with these predictions (see Table 3).

Table 3 is a summary of the dynamical properties of the poor clusters. Column (1) is the cluster name, column (2) the number of galaxies in sample A, and column (3) the number of galaxies in samples A and B taken together. Columns (4) and (5) contain the mean galactocentric velocity and the line-of-sight velocity dispersion for sample A. Columns (6) and (7) contain the corresponding quantities for the combined samples A and B. Columns (8) and (9) are mass-to-light ratios from the virial theorem and projected mass estimates, respectively. These estimates are based on sample A in each case. The numbers in parentheses are analytic estimates (lower limits in the case of the virial theorem) of the errors. No error in $L_{B(0)}$ is included in these error estimates (see § V*a* for further discussion).

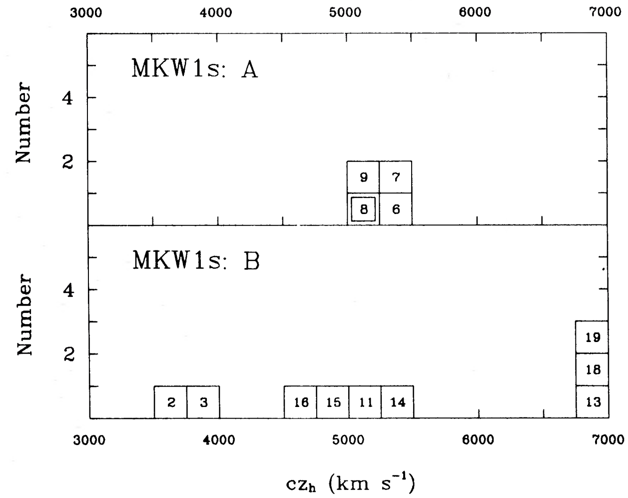

FIG. 2.—Velocity histogram for MKW 1s. Bins are 250 km s^{-1}. Numbers in the boxes are the 5° identifications given in Table 1. A double box marks the D galaxy.

i) *MKW 1s*

Of the eight galaxies in the Zwicky catalog within 1° (0.9 Mpc) of the bright galaxy 0917+0116, four are background to the cluster; the poor get poorer. The velocity histogram in Figure 2 indicates contamination in the 5° region (sample B), but none within the 1° sample. For the four galaxies in sample A, the velocity dispersion $\sigma_{\mathrm{A}} = 66\,(+89, -24)$ km s^{-1} is small. Nonparametric tests (Yahil and Vidal 1977) of the combined sample A + B show that the velocity distribution is inconsistent with a Gaussian because of the four galaxies in the tails of the distribution. (a, $\alpha < 0.05$; w, $\alpha < 0.10$). If we remove these four galaxies, the remaining eight galaxies give $\sigma_{\mathrm{A+B}} = 250$ $(+116, -48)$ km s^{-1}, an upper limit to the dispersion. The mass-to-light ratios (using only the four galaxies in sample A) are small and uncertain. The errors are large because of the undersampled velocity distribution. The virial mass-to-light ratio based on the upper limit to the dispersion ($\sigma_{\mathrm{A+B}} = 250$ km s^{-1}) is $M_{\mathrm{vt}}/L_{B(0)} = 440\ M_\odot/L_\odot$.

ii) *AWM 1*

There are 56 galaxies in the 5° region with measured redshifts. Of these, 15 are foreground with $cz_h < 6500$ km s^{-1}, and six have velocities $cz_h > 10{,}500$ km s^{-1}. Figure 3 is the velocity

TABLE 3

VELOCITY DISPERSION AND MASS-TO-LIGHT RATIOS[a]

Cluster (1)	N_{A} (2)	$N_{\mathrm{A+B}}$ (3)	$\langle cz_g \rangle_{\mathrm{A}}$ (km s^{-1}) (4)	σ_{A} (km s^{-1}) (5)	$\langle cz_g \rangle_{\mathrm{A+B}}$ (km s^{-1}) (6)	$\sigma_{\mathrm{A+B}}$ (km s^{-1}) (7)	$M_{\mathrm{vt}}/L_{B(0)}$ ($M_\odot/L_\odot$) (8)	$M_{\mathrm{pm}}/L_{B(0)}$ ($M_\odot/L_\odot$) (9)
				Complete				
MKW 1s	4	8	5024 ± 38	66 (+89, −24)	5017 ± 93	250 (+116, −48)	22 ± 21(6)	134 ± 119(108)
AWM 1	12	...	8249 ± 96	317 (+97, −51)	...	...	120 ± 49(25)	241 ± 89(101)
AWM 7	20	33	5404 ± 199	865 (+183, −112)	5300 ± 150	849 (+130, −89)	1120 ± 273(195)	1130 ± 292(362)
				Incomplete				
MKW 1	8	15	5931 ± 94	251 (+117, −50)	5937 ± 63	233 (+61, −35)	125 ± 57(29)	94 ± 49(49)
MKW 4	13	...	6093 ± 205	708 (+204, −109)	...	...	462 ± 142(92)	443 ± 156(179)
MKW 12 ...	11	...	5997 ± 68	216 (+71, −36)	...	...	83 ± 28(17)	57 ± 21(25)
AWM 3	8	16	4596 ± 138	369 (+172, −72)	4656 ± 107	414 (+102, −59)	457 ± 206(105)	1500 ± 810(784)

[a] Errors in the mass-to-light ratios include only the error in the mass. Numbers in parentheses in cols. (8) and (9) are analytically calculated lower limits to the error in the case of the virial theorem and analytically calculated errors in the case of the projected mass.

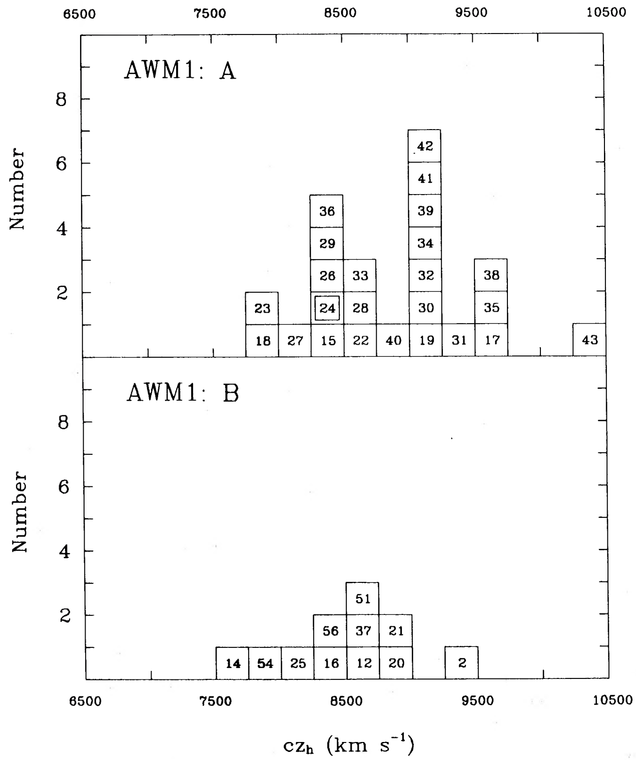

FIG. 3.—Velocity histogram for AWM 1. Bins are 250 km s^{-1}.

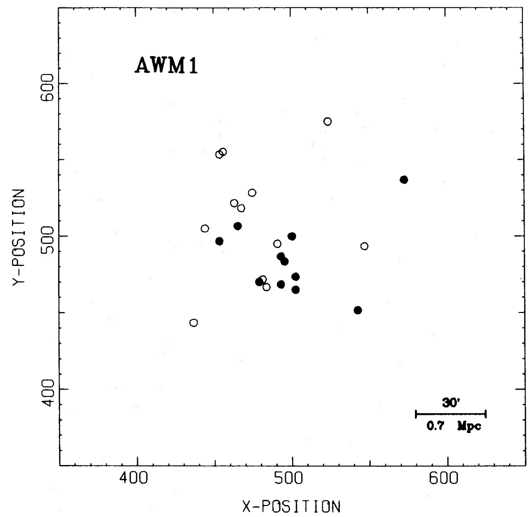

FIG. 4.—Positions for galaxies in AWM 1. Closed circles are galaxies with $cz_h < 9000$ km s^{-1} (subsample A1); open circles are galaxies with $cz_h > 9000$ km s^{-1} (subsample A2).

histogram for the 35 galaxies in the velocity range $6500 < cz_h < 10{,}500$ km s^{-1}. The 24 galaxies in sample A include a member of a binary system not listed in the Zwicky catalog (NGC 2807B, SW of NGC 2807A). No redshift was measured for the galaxy 0910+2035.

The two pronounced peaks in the velocity distribution (sample A) suggest contamination which can be demonstrated by using the spatial and velocity information together. We examine the evidence for correlation of velocities with position by dividing sample A at 9000 km s^{-1}; the 12 galaxies with $cz_h < 9000$ km s^{-1} are subsample A1, the 12 galaxies with $cz_h > 9000$ km s^{-1} are subsample A2. Figure 4 is a plot of the galaxy positions (in arbitrary X, Y coordinates) for these subsamples. The centroid of subsample A2 is offset by $\sim 20'$ (0.5 Mpc) to the NE of the centroid of A1. More precisely, for subsample A1, $\bar{x} = 499 \pm 9$, $\bar{y} = 484 \pm 6$; for subsample A2, $\bar{x} = 476 \pm 9$, $\bar{y} = 509 \pm 11$. We test the significance of this offset with a χ^2 test (Faber and Dressler 1977). The result is $\chi^2 = 7.3$. For two degrees of freedom, the probability of obtaining $\chi^2 > 7.3$ is only $\sim 3\%$. The two subsamples are separated in space as well as velocity. We derive dynamical parameters from subsample A1, which includes the D galaxy.

iii) *AWM 7*

The dynamical analysis for this system is clouded because AWM 7 is only 4°.5 from the core of the Perseus cluster. AWM 7 is one of several condensations in the extensive Perseus Supercluster (see Fig. 5).

The list of galaxies in AWM 7 (Table 1) is for the 1° (0.9 Mpc) field where we have a nearly complete redshift sample. No redshift was measured for IGC 266 because of a superposed bright star. There are ~ 200 galaxies with measured redshifts in the 5° region which includes much of the Perseus Cluster (Kent and Sargent 1983).

Figure 6 is the velocity histogram for the 33 galaxies in the 1° sample with $3500 < cz_h < 7500$ km s^{-1}. If we sort the 33 galaxies into two groups according to their projected radial distance from NGC 1129, we reproduce the apparent increase in velocity dispersion noted by Hintzen (1980). For the 16 galaxies within 0.25 Mpc, $\langle cz_g \rangle = 5355 \pm 177$ km s^{-1}, and $\sigma_r = 684\ (+169, -97)$ km s^{-1}. The mean and dispersion of the 17 galaxies between 0.25–0.9 Mpc from NGC 1129 are $\langle cz_g \rangle = 5219 \pm 254$ km s^{-1}, and $\sigma_r = 1015\ (+240, -140)$ km s^{-1}. Hintzen argues that this increase in velocity dispersion is *not* due to contamination because (1) the mean velocity is the same for both samples, and (2) the velocities of the galaxies at large radii are uncorrelated with their estimated magnitudes.

Within $\sim 40'$ of the Perseus Cluster center the velocity dispersion profile is flat or slowly rising. The dispersion falls to ~ 600 km s^{-1} at $\sim 3°$ from the cluster center (Kent and

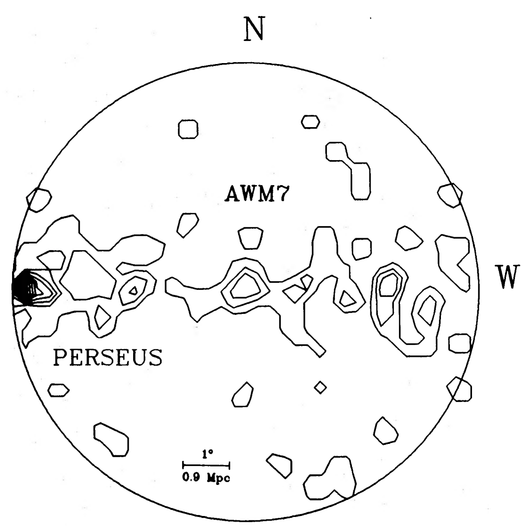

FIG. 5.—Surface number density contour map for galaxies in the region of AWM 7. Note the central region of the Perseus Cluster $\sim$4°.5 to the east of AWM 7. AWM 7 is clearly flattened along the plane of the Perseus Supercluster. The lowest contour corresponds to about two galaxies per $30' \times 30'$ bin, the highest contour is 16 galaxies per bin. Contours are linearly spaced.

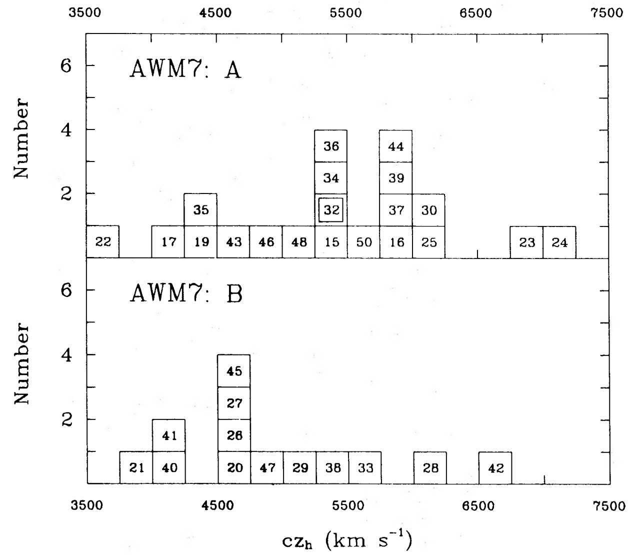

FIG. 6.—Velocity histogram for AWM 7. Bins are 250 km s^{-1}. Only galaxies in the 1° region are shown.

Sargent 1983). A mere superposition of AWM 7 and Perseus Cluster members cannot, therefore, explain the radially increasing velocity dispersion in AWM 7. A deeper *complete* velocity sample may determine whether the larger dispersion could be due to a superposition of condensations in the Perseus Supercluster (e.g., Bothun *et al.* 1983).

Estimation of the mass-to-light ratio for AWM 7 is further complicated by the large and variable galactic reddening in the region. The color excess $E_{B-V} \approx 0.1$ corresponds to $A_B \approx 0.4$ mag (Burstein and Heiles 1982). The formal mass-to-light ratios we obtain for AWM 7 are quite high: $M_{\rm vt}/L_{B(0)} = 1120 \pm 290\ M_\odot/L_\odot$ and $M_{\rm pm}/L_{B(0)} = 1130 \pm 290\ M_\odot/L_\odot$. If we use the dispersion for the central 0.25 Mpc region, the virial mass-to-light ratio decreases by a factor of ~ 1.6, to $M_{\rm vt}/L_{B(0)} \approx 700\ M_\odot/L_\odot$.

b) *Analysis of Incomplete Samples*

Figure 7 is a set of cone diagrams in right ascension and heliocentric velocity (cz_h) for the four systems MKW 1, MKW 4, MKW 12, and AWM 3. The dashed lines outline the subsample of velocities within ± 2000 km s^{-1} of the D galaxy. Galaxies with extreme velocities have been removed.

On the basis of the spatial and velocity information we select two mutually exclusive subsamples for further analysis. Both subsamples of galaxies lie within the dashed lines on the cone diagrams. The subsamples A and B, are as follows:

A: Galaxies projected *within* 1.5 Mpc of the D galaxy (using the velocity of this galaxy to set the metric scale).

B: Galaxies projected *outside* the 1.5 Mpc radius but *within* the bounds of the 5° region.

The spatial cutoff $R = 1.5$ Mpc is roughly twice the median size for nearby groups of galaxies in the CfA redshift survey (Huchra and Geller 1982) and is an Abell radius for $H_0 = 100$ km s^{-1} Mpc^{-1} (Abell 1958). We use sample B to ferret out interlopers in sample A.

The expected fractional contamination is greater for these poor clusters than for richer clusters. This problem is particularly severe when a poor cluster is located near some other galaxy-rich field. We need both the spatial and velocity information to differentiate between interlopers and members of the MKW-AWM system. In at least one case sample B adds confidence to this rejection by identifying other systems of galaxies which extend into region A. Frequently there are galaxies in sample B which clearly lie in the velocity range of the MKW-AWM system. In this case we combine the velocities in the larger field with those in sample A to set an upper limit on the velocity dispersion.

Because of the incomplete sampling, the calculation of cluster luminosity requires several intermediate corrections. We define L_m to be the total luminosity for the N_m cluster members assigned from sample A with $m_{B(0)} \leq 15.7$ (Table 2, col. [4]), and L_i to be the total luminosity for the N_i interlopers with $m_{B(0)} \leq 15.7$ (Table 2, col. [5]). The fraction of luminosity contributed by *members* brighter than $m_{B(0)} = 15.7$ is

$$f_1 = \frac{L_m}{L_m + L_i} \tag{4}$$

(Table 2, col. [7]). The luminosity contributed to the system by galaxies in the Zwicky catalog is then

$$L_{B(0)} = L_m + f_1 L_u , \tag{5}$$

where L_u is the total luminosity of galaxies in the Zwicky catalog sample *without* measured redshifts (Table 2, col. [6]). We use the mean velocity of the cluster in obtaining estimates of the intrinsic luminosities of these galaxies. We correct for galactic absorption, K-dimming, and for the contribution of galaxies fainter than $m_{B(0)} = 15.7$. This procedure is probably somewhat biased because apparently brighter galaxies are more likely to have measured redshifts. If the contamination is due primarily to background objects, the luminosity will be overestimated, and the mass-to-light ratio underestimated. Although limited, this estimation technique is clearly *less* biased than summing the luminosity of all the Zwicky galaxies in the field.

i) *MKW 1*

There are 40 galaxies with redshift measurements in the 5° sample for MKW 1 (Table 1): 14 have $cz_h < 4000$ km s^{-1}, and nine have $cz_h > 8000$ km s^{-1}. Figure 8 is a velocity histogram for the 17 galaxies with $4000 < cz_h < 8000$ km s^{-1}. All eight galaxies in sample A are probable cluster members. The galaxies in the central peak of the histogram for sample B may also be cluster members; galaxies 2 and 8 are likely interlopers. The mean and dispersion for the sample A + B (15 galaxies; 2, 8 deleted) are $\langle cz_g \rangle = 5937 \pm 63$ km s^{-1} and $\sigma_{\rm A+B} = 233$ $(+61, -35)$, completely consistent with the estimates from sample A alone.

ii) *MKW 4*

There are 53 galaxies with measured redshifts in the 5° field for MKW 4 (Table 1): 21 galaxies have $cz_h < 4000$ km s^{-1} (most are associated with the Virgo Supercluster which is foreground to MKW 4), and nine have $cz_h > 8000$ km s^{-1}. Figure 9 is the velocity histogram for the 23 galaxies with $4000 < cz_h < 8000$ km s^{-1}. The 13 galaxies in sample A are spread out in velocity between $4750 < cz_h < 7250$ km s^{-1}. This spread suggests either a large velocity dispersion or severe contamination. Neither sample A nor B enables discrimination between cluster members and interlopers.

iii) *MKW 12*

MKW 12 is the "nearby" Zwicky cluster Zw 1400+0949. There are 75 galaxies with measured redshifts in the region (Table 1): 11 have $cz_h < 4000$ km s^{-1}, and 13 have redshifts

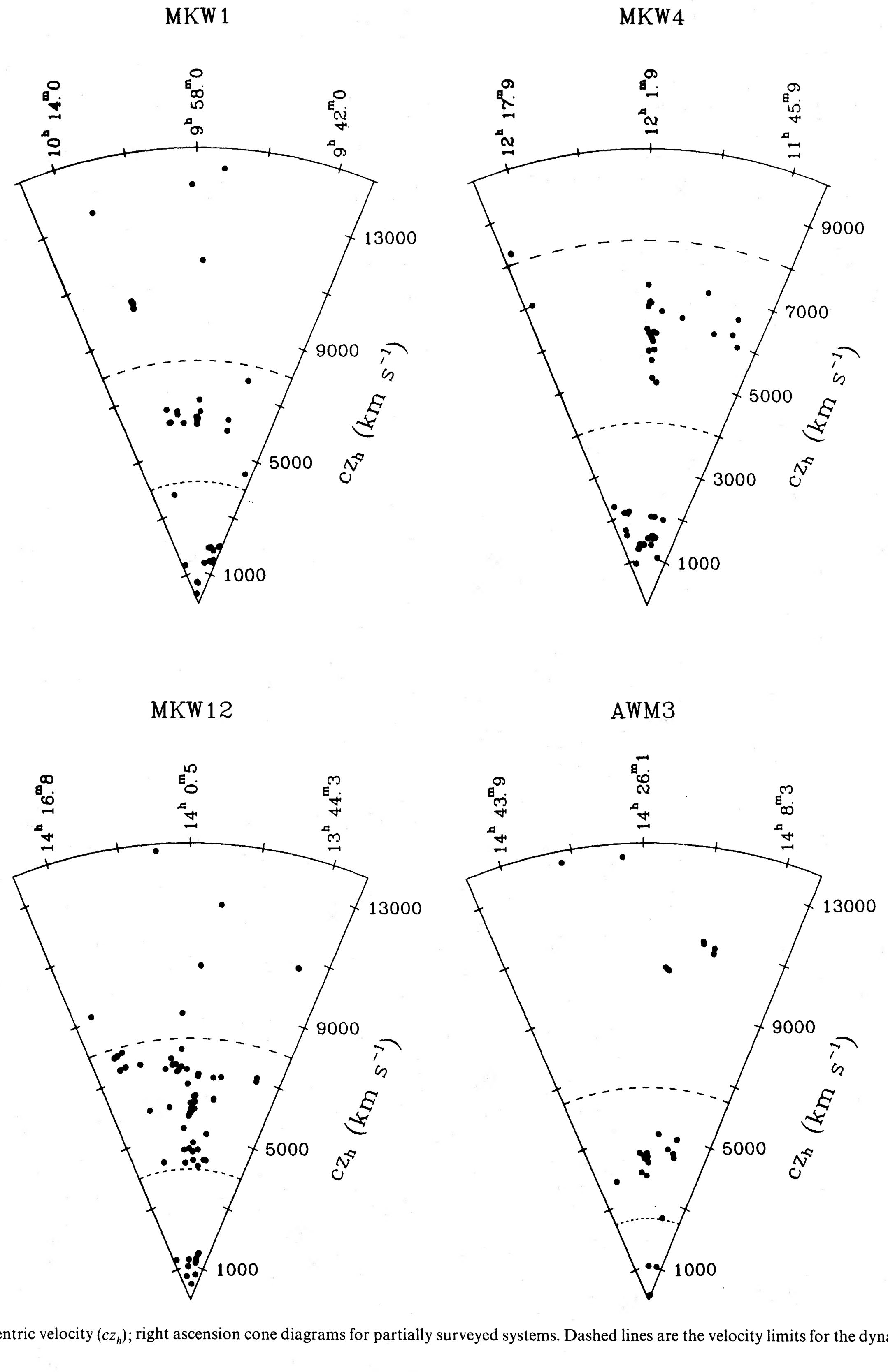

FIG. 7.—Heliocentric velocity (cz_h); right ascension cone diagrams for partially surveyed systems. Dashed lines are the velocity limits for the dynamical analysis.

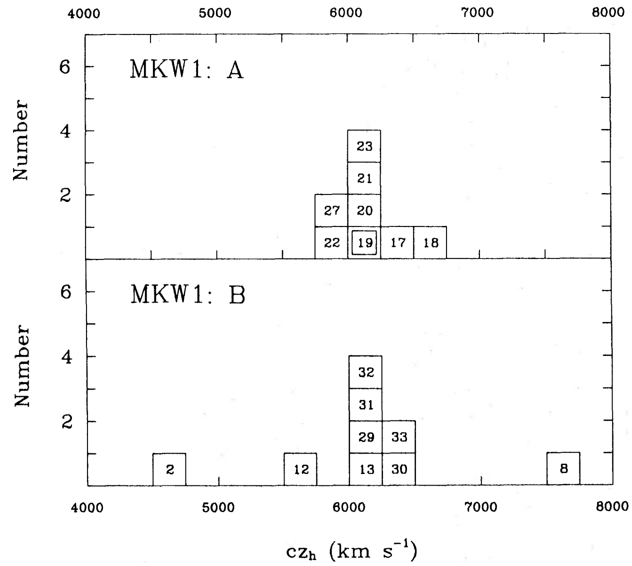

FIG. 8.—Velocity histogram for MKW 1. Bins are 250 km s^{-1}.

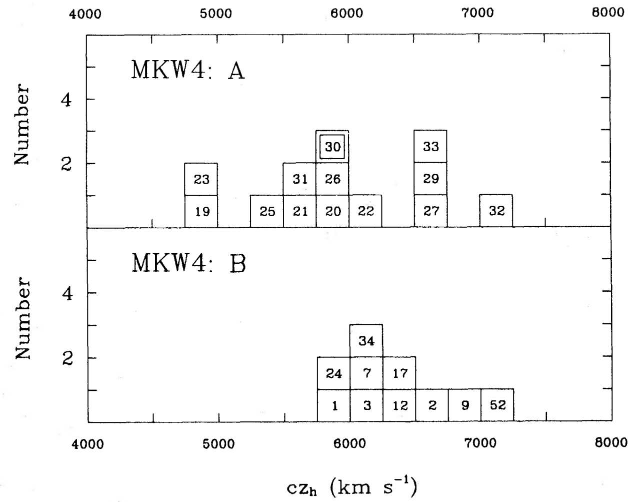

FIG. 9.—Velocity histogram for MKW 4. Bins are 250 km s^{-1}.

$cz_h > 8000$ km s^{-1}. Figure 10 is a velocity histogram for the 51 galaxies with $4000 < cz_h < 8000$ km s^{-1}. The histogram for sample A is trimodal and suggests severe contamination. We assign the three obvious peaks in the distribution to the subsamples A1, $4000 < cz_h < 5000$ km s^{-1}; A2, $5500 < cz_h < 6500$ km s^{-1}; and A3, $6500 < cz_h < 7250$ km s^{-1}. The correspondence of peaks in samples A and B is further evidence that subsamples A1 and A3 are not associated with MKW 12. For the 11 galaxies in subsample A2, we obtain $\langle cz_g \rangle = 5997 \pm 68$ km s^{-1} and $\sigma_A = 216\,(+71, -36)$. The mean velocities of subsamples A1 and A3 are displaced from that of A2 by $> 3\sigma_A$. Figure 11 shows that the galaxies in A1 and A3 are also located outside the central region which contains almost exclusively galaxies in A2. For this system, the value $f_1 = 0.48$ (Table 2) reflects the severe contamination.

iv) *AWM 3*

There are 44 galaxies in the region with measured redshifts (Table 1): three are foreground with $cz_h < 2500$ km s^{-1}, and 24 have $cz_h > 6500$ km s^{-1}. AWM 3 is a condensation in the "nearby" Zwicky cluster Zw 1424+2613. Figure 12 is the velocity histogram for the 17 galaxies in the range $2500 < cz_h < 6500$ km s^{-1}. The projected mass estimate (Table 3) is so much larger than the virial estimate because the galaxies (15 and 22) with velocities most deviant from the mean are located at the largest radii.

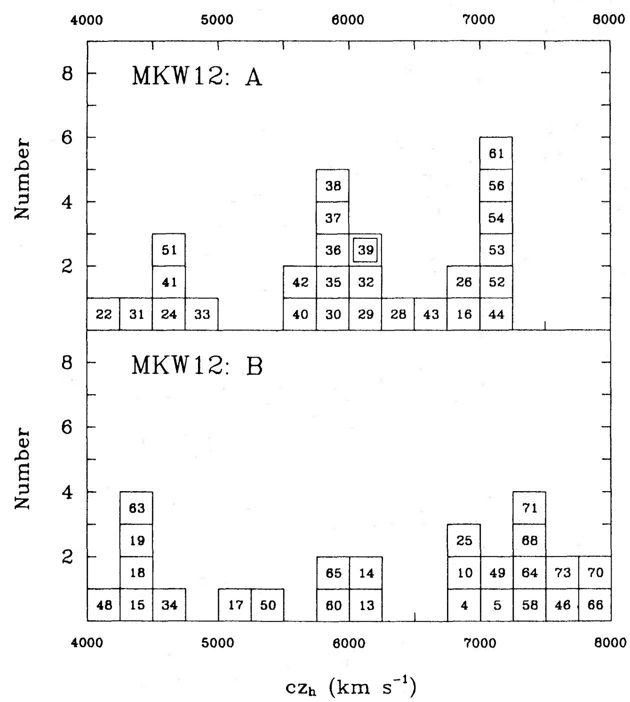

FIG. 10

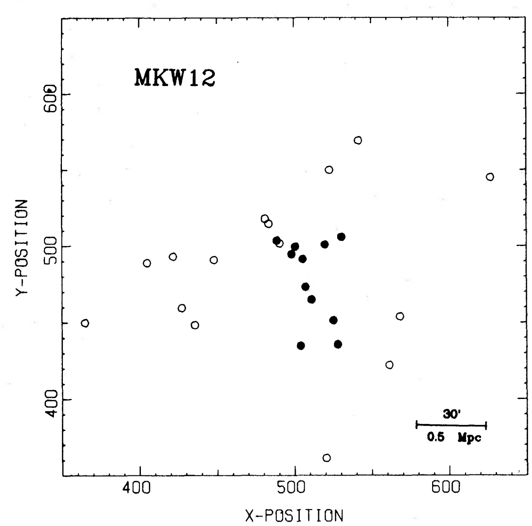

FIG. 11

FIG. 10.—Velocity histogram for MKW 12. Bins are 250 km s^{-1}.

FIG. 11.—Positions for galaxies in MKW 12. Closed circles are galaxies with $5500 < cz_h < 6500$ km s^{-1} (A2); open circles are galaxies in the velocity ranges $4000 < cz_h < 5000$ km s^{-1} (A1) and $6500 < cz_h < 7250$ km s^{-1}(A3).

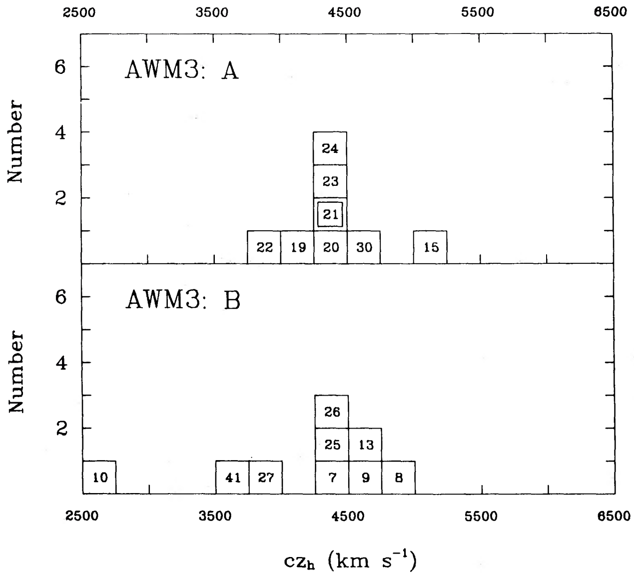

FIG. 12.—Velocity histogram for AWM 3. Bins are 250 km s^{-1}.

c) The Significance of the D Galaxy

MKW and AWM selected poor clusters for the distinctive morphology of the D galaxies. X-ray observations suggest that the D galaxies lie at the bottom of the cluster potential wells. The velocity data provide independent support of this conclusion.

To test the kinematic significance of the D galaxies, we apply a Spearman rank correlation test (Lehmann 1975) to the velocity data. In each cluster, we determine the mean velocity for all cluster members (sample A) *except* the D. We then rank the velocities according to their absolute difference from this mean. We rank the same set of velocities by their absolute difference from the velocity of the D galaxy. A comparison of the two sets of ranks gives the rank correlation coefficient, r_s. The value of this statistic tests whether the D galaxy is a good *predictor* of the mean velocity of the system. Note that the identification of the poor clusters and the selection of galaxies for observation do not bias the velocity of the D galaxy toward the mean of the system. For all the clusters (except MKW 1s), the velocity of the D galaxy *is* an excellent predictor of the sample mean ($\alpha < 0.05$ in each case). The contrary result for MKW 1s is hard to evaluate because of the extremely small sample size.

Are the D galaxies closer to the sample mean velocity than any other galaxy randomly drawn from the distributions? We answer this question by assembling a single data set which includes all member galaxies in the clusters (except MKW 1s). The absolute velocity difference of each galaxy from its cluster mean is normalized by the cluster velocity dispersion and then ranked. The hypothesis that the D galaxies are drawn at random from the full list of ranks is rejected at the $\alpha = 0.025$ level (one-sided KS test). Including the data from MKW 1s decreases the significance to $\alpha = 0.0875$. The D galaxies in MKW-AWM poor clusters lie at rest in the local potential well.

IV. SPECTROSCOPIC COMPARISONS OF X-RAY cDs

Figure 13 shows medium resolution digital spectra (6–7 Å) near Hα for the D or cD galaxies in a number of X-ray clusters with cooling flows (Heckman 1981; Cowie *et al.* 1983). These spectra were obtained with the "*Z*-machine" on the 1.5 m telescope at Whipple Observatory through a 12″.5 × 3″.2 slit. The full wavelength region coverage is nominally 4500–7000 Å. The spectra plotted in Figure 13 are in raw counts over the wavelength region 6200–6800 Å in the rest frame of the galaxy. The emission-line system Hα-[N II] (λ6583) is indicated for each spectrum. We roughly quantify the line emission in Hα-[N II] relative to the optical continuum by obtaining equivalent widths for the three lines taken together (Table 4). Column (1) of Table 4 is the cluster name, column (2) the summed Hα-[N II] emission reported by Cowie *et al.* (1983) in ergs per second, column (3) our measured equivalent widths in angstroms, and column (4) the slit dimension in kiloparsecs at the galaxy redshift. Column (5) is the ratio of the Hα-[N II] luminosities for each galaxy relative to that for Perseus (NGC 1275), and column (6) is the corresponding ratio of Hα-[N II] equivalent widths. The spectrum of the cD in A1795 cuts off too blueward to derive an equivalent width. Because the Hα-[N II] features of MKW 4 and AWM 7 are not strong enough to measure accurate equivalent widths, we estimate an upper limit for the rms power over the region of Hα-[N II].

The spectra of Figure 13 and equivalent widths of Table 4 show that there is less emission due to cooling flows onto the cores of NGC 4073 in MKW 4 or NGC 1129 in AWM 7 than there is for Perseus, M87, or A1795. The Hα-[N II] emission is comparable with that for A85 or A496 and is consistent with the 2–10 keV X-ray luminosities estimated for MKW 4 and AWM 7 (1.3×10^{43} and 1.6×10^{44} ergs s^{-1}, respectively) from the 0.5–4.5 keV luminosities and temperatures (KCC). The line emission in our spectrum of A2199 is much stronger than reported by Cowie *et al.* (1983). Their measurements limited the sum of extended and nuclear Hα-[N II] emission to less than 5×10^{39} ergs s^{-1}. The expected ratio of equivalent widths (Table 4) would then be ~0.01. We measure an equivalent

TABLE 4

Hα-[N II] EQUIVALENT WIDTHS OF D AND cD GALAXIES

Cluster (1)	L(Hα + [N II]) (ergs s^{-1}) (2)	Hα-[N II] Equivalent Width (3)	Slit Width (kpc) (4)	L(Hα + [N II]) / L(Hα + [N II])$_{\rm NGC\,1275}$ (5)	Equivalent Width / Equivalent Width$_{\rm NGC\,1275}$ (6)
Perseus	230×10^{44}	−125	3.1	1	1
Virgo	...	−15	1.3	...	0.12
A85	10	−7	9.3	0.04	0.06
A496	13	−13	5.7	0.06	0.10
A1795	41	...	10.5	0.18	...
A2199	2	−28	5.4	0.01	0.22
MKW 4	...	> −8	3.5	...	<0.06
AWM 7	...	> −9	3.1	...	<0.07

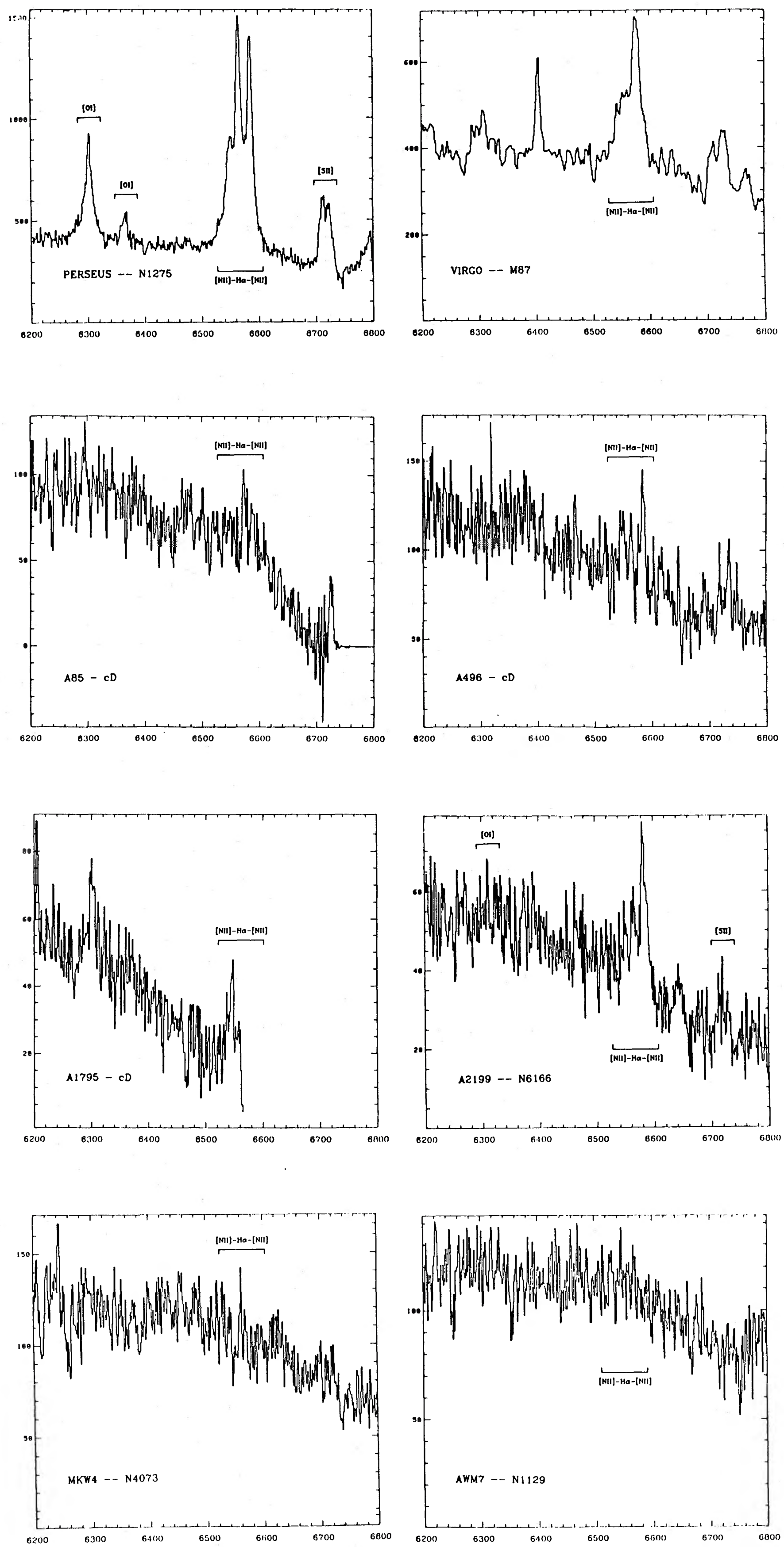

FIG. 13.—Medium resolution digital spectra of the D or cD galaxies in clusters with cooling flows. Vertical axis is raw counts; the wavelength scale is for the rest frame of the galaxy. Region of the emission system Hα-[N II] is indicated.

width ratio ~ 0.2 (col. [6], Table 4), a factor of 20 greater. The origin of this discrepancy is not clear.

V. DISCUSSION

A combination of our measurements and those in the literature yields velocities for a total of 76 member galaxies in seven MKW-AWM poor clusters. For all but one of the systems (MKW 1s), we have eight or more velocity measurements. As a comparison, only 20% of the loose groups in the CfA redshift survey (Geller and Huchra 1983) have at least this number of velocity measurements. In the three complete samples we have redshifts for *all* member galaxies to 0.5–1.5 mag fainter than the knee of the galaxy luminosity function. The fractional sampling is thus greater than for many rich clusters. These data therefore provide a basis for consistent estimates of the physical parameters of the systems.

a) Mass-to-Light Ratios

We have estimated the masses of the clusters by applying both the virial theorem and the projected mass method. For all seven poor clusters, the two estimates agree within 1.5 σ (Table 3). The fractional error in $M/L_{B(0)}$ is equal to the fractional error in M alone: no error in $L_{B(0)}$ is included in these estimates. There are a number of sources of error in $L_{B(0)}$. Uncertainty in the galaxy luminosity function affects the correction applied for galaxies fainter than the survey limit. The corrections for incompleteness (Table 2) are also uncertain and possibly somewhat biased. Finally, the fractional errors in individual galaxy magnitudes are $\lesssim 30\%$. The typical fractional error in $L_{B(0)}$ from these factors taken together is $\sim 20\%$. Systematic error due to incompleteness of the Zwicky catalog near the magnitude limit may well dominate over the statistical error. Better photometric data are needed for studies of systems of galaxies.

The jacknife is a powerful tool for making an internal error estimate. It reproduces the expected results for the projected mass estimator (Table 3; col. [9]). Because of the unpleasant statistical properties of the virial theorem estimator, errors are rarely quoted. Only a lower limit to the error can be calculated analytically (Bahcall and Tremaine 1981). The jacknife gives a much needed measure of the typically large actual fractional error in the virial theorem estimate. The results in Table 3 are typically a factor of 2 or 3 times the lower limit. Tests of the jacknife on simulated data are needed.

b) Cluster Characteristics

The poor clusters fall into two categories: the most X-ray luminous clusters (MKW 4 and AWM 7) have velocity dispersions of order 700 km s^{-1}, and mass-to-light ratios of 400 $M_\odot/L_\odot$ or more; the other five clusters have velocity dispersions of 370 km s^{-1} or less, and four of the five have mass-to-light ratios of 250 $M_\odot/L_\odot$ or less. For the fifth of these, AWM 3, the mass-to-light ratio is large but uncertain. The binding masses inferred from isothermal models for the X-ray emitting gas (KCC) agree well with the masses determined from the optical data. KCC find that 10%–20% of the mass in the systems is in the form of hot gas.

All seven clusters have crossing times less than $0.2H_0^{-1}$. The typical scale of these systems, measured by the mean pair-wise separation of the members, is ~ 0.5 Mpc. The D galaxies in MKW 4 and AWM 7 contribute $\sim 20\%$ of the total luminosity of the poor cluster; for the other poor clusters, the contribution of the D is only 5%–10% of the total.

The poor clusters have a wide range of mass densities. At one extreme, the mass density of MKW 1s (scaled to a radius of 1.5 Mpc) is $\sim 1\%$ of the density for the Coma cluster (2.9×10^{-27} g cm^{-3}; Kent and Gunn 1982). AWM 7 has a mass density approaching that of Coma. The remaining systems have mass densities $\sim 10\%$ of Coma. Beers and Geller (1983) evaluate surface number densities for clumps in rich clusters with associated D or cD galaxies. The range of surface number density spanned by the MKW-AWM poor clusters is the same as for the subclusters.

c) Characteristics of Individual Galaxies

The velocity data demonstrate, in a model-independent way, that the D galaxies in poor clusters lie at or near the center of mass of the system. This kinematic result supports the X-ray evidence for cooling flows onto the D galaxies in MKW 4 and AWM 7 (KCC).

The strengths of the optical emission line system Hα-[N II] for NGC 4073 and 1129 are marginally consistent with the emission from cD galaxies in clusters of comparable X-ray luminosity. Although luminous halos have not been detected (Thuan and Romanishin 1981; Morbey and Morris 1983), the central densities in MKW 4 and AWM 7 are just sufficient for tidal stripping to occur. Halos of low-mass stars could also form out of the cooling flow (Fabian, Nulsen, and Canizares 1982).

The remaining poor clusters which were observed in the X-ray show no evidence for cooling flows. These clusters also have central galaxy densities which are too low for collisional stripping to be important. The low velocity dispersions ($\lesssim 370$ km s^{-1}) for five of the poor clusters favor the merger picture for formation of the central galaxies (Carnevali, Cavaliere, and Santangelo 1981; Tremaine 1981).

We thank the staff at the Whipple Observatory, especially Jim Peters and Ed Horine, for expiditious redshift observations. Susan Tokarz assisted in the data reduction. We also thank the anonymous referee for encouraging us to shorten and tighten the paper. This research was supported by NASA grant NAGW-201 and the Smithsonian Institution.

REFERENCES

Abell, G. O. 1958, *Ap. J. Suppl.*, **3**, 211.
Albert, C. E., White, R. A., and Morgan, W. W. 1977, *Ap. J.*, **211**, 309 (AWM).
Bahcall, N. A. 1980, *Ap. J. (Letters)*, **238**, L117.
Bahcall, J., and Tremaine, S. 1981, *Ap. J.*, **244**, 805.
Beers, T. C. 1983, Ph.D. thesis, Harvard University.
Beers, T. C., and Geller, M. J. 1983, *Ap. J.*, **274**, 491.
Bohuski, T., Fairall, A., and Weedman, D. 1978, *Ap. J.*, **221**, 776.
Bothun, G. D., Geller, M. J., Beers, T. C., and Huchra, J. P. 1983, *Ap. J.*, **268**, 47.
Burstein, D., and Heiles, C. 1982, *A.J.*, **87**, 1165.
Canizares, C. R., Steward, G. C., and Fabian, A. C. 1983, *Ap. J.*, **272**, 29.
Carnevali, P., Cavaliere, A., and Santangelo, P. 1981, *Ap. J.*, **249**, 449.
Colla, G., *et al.* 1975, *Astr. Ap. Suppl.*, **20**, 1.
Cowie, L. L., Hu, E. M., Jenkins, E. B., and York, D. G. 1983, preprint.
Coleman, G. D., Wu, C., and Weedman, D. 1980, *Ap. J. Suppl.*, **43**, 393.
Danese, L., De Zotti, G., and di Tullio, G. 1980, *Astr. Ap.*, **82**, 322.
Davis, M., and Huchra, J. P. 1982, *Ap. J.*, **254**, 437.
de Vaucouleurs, G., and de Vaucouleurs, A. 1964, *Reference Catalog of Bright Galaxies* (Austin: University of Texas Press).
Diaconis, P., and Efron, B. 1983, *Sci. Am.*, **248**, 116.
Faber, S. M., and Dressler, A. 1977, *A.J.*, **82**, 187.
Fabian, A. C., Nulsen, P. E. J., and Canizares, C. R. 1982, *M.N.R.A.S.*, **201**, 933.
Geller, M. J., and Huchra, J. P. 1983, *Ap. J. Suppl.*, **52**, 61.

Heckman, T. 1981, *Ap. J.* (*Letters*), **250**, L59.
Hintzen, P. 1980, *A.J.*, **85**, 626.
Huchra, J. P. 1976, *A.J.*, **81**, 952.
———. 1984, in preparation.
Huchra, J. P., and Geller, M. J. 1982, *Ap. J.*, **257**, 423.
Huchra, J. P., Davis, M., Latham, D. W., and Tonry, J. 1983, *Ap. J. Suppl.*, **52**, 89.
Kent, S. M., and Gunn, J. E. 1982, *A.J.*, **87**, 945.
Kent, S. M., and Sargent, W. L. W. 1983, *A.J.*, **88**, 697.
Kriss, G. A. 1983, private communication.
Kriss, G. A., Cioffi, D. F., and Canizares, C. R. 1983, *Ap. J.*, **272**, 439.
Kriss, G. A., Canizares, C. R., McClintock, J. E., and Feigelson, E. D. 1980, *Ap. J.* (*Letters*), **235**, L61.
Latham, D. W. 1982, in *IAU Colloquium 67, Instrumentation for Astronomy with Large Optical Telescopes*, ed. Colin M. Humphries (Dordrecht: Reidel), p. 259.
Lehmann, E. L. 1975, *Nonparametrics: Statistical Methods Based on Rank* (San Francisco: Holden-Day).
Morbey, C., and Morris, S. 1983, *Ap. J.*, **274**, 502.
Morgan, W. W., Kayser, S., and White, R. A. 1975, *Ap. J.*, **199**, 545 (MKW).
Palumbo, G. G. C., Tanzella-Nitti, G., and Vettolani, P. 1983, *Catalogue of Radial Velocities of Galaxies* (New York: Gordon & Breach).
Sandage, A. 1973, *Ap. J.*, **183**, 711.
Schwartz, D. A., *et al.* 1980, *Ap. J.* (*Letters*), **238**, L53.
Stauffer, J., and Spinrad, H. 1978, *Pub. A.S.P.*, **90**, 20.
———. 1980, *Ap. J.*, **235**, 347.
Thomas, J. C., and Batchelor, D. 1978, *A.J.*, **83**, 1160.
Thuan, T. X., and Romanishin, W. 1981, *Ap. J.*, **248**, 439.
Thuan, T. X., and Seitzer, P. 1979, *Ap. J.*, **231**, 327.
Tremaine, S. 1981, in *The Structure and Evolution of Normal Galaxies*, ed. S. M. Fall and D. Lynden-Bell (Cambridge: Cambridge University Press), p. 67.
Yahil, A., and Vidal, N. V. 1977, *Ap. J.*, **214**, 347.
Zwicky, F., Herzog, E., Wild, P., Karpowicz, M., and Kowal, C. 1961–1968, *Catalog of Galaxies and of Clusters of Galaxies*, Vols. **1–6** (Pasadena: California Institute of Technology).

T. C. Beers: Astronomy Department, Caltech, 1201 E. California Blvd., Pasadena, CA 91125

R. J. Davis, M. J. Geller, J. P. Huchra, and D. W. Latham: Center for Astrophysics, 60 Garden Street, Cambridge, MA 02138